DOI: 10.1002/ejic.200800598

A Carbazole-Containing Difunctional Ru^{II} Complex That Functions as a pH-Induced Emission Switch and an Efficient Sensitizer for Solar Cells

Su-Hua Fan,[a] Ke-Zhi Wang,*[a] and Wei-Chun Yang[a]

Keywords: Ruthenium / Phenanthroline / Carbazole / Protonation / Emission switch / Solar cells / Sensitizers / Mesoporous materials

A heteroleptic ruthenium(II) complex of [Ru(Hecip)(Hdcbpy)$(NCS)_2]^-$·$[N(C_4H_9)_4]^+$ (where Hecip = 2-(9-ethyl-9*H*-carbazol-3-yl)-1*H*-imidazo[4,5-*f*][1,10]phenanthroline and Hdcbpy = monodeprotonated 2,2′-bipyridyl-4,4′-dicarboxylic acid) has been synthesized and characterized by elementary analysis, cyclic voltammetry, MALDI-TOF mass spectrometry, and ^1H NMR, IR, UV/Vis absorption, and emission spectroscopy. The ground- and excited-state acid–base properties of the complex have been studied by means of UV/Vis absorption spectrophotometric and spectrofluorimetric titrations in a Britton–Robinson/DMF (v/v, 4:1) buffer solution. The complex was found to act as pH-induced off-on-off/on-off-on-off-type emission switch, when excited at 530/470 nm, with a protonation/deprotonation reaction taking place near the physiological pH range. The performance of the complex-sensitized TiO_2 nanocrystalline solar cell with 0.05 M I_2 and 0.5 M LiI in 50 % acetonitrile and 50 % propylene carbonate (PC) as the electrolyte solution and a platinum film as the counter electrode has also been studied, and was compared to that of the *cis*-$[Ru(H_2dcbpy)_2(NCS)_2]$ (N3)-sensitized solar cell under the same experimental conditions.

Introduction

Dye-sensitized solar cells (DSSCs) based on mesoporous nanocrystalline TiO_2 films have attracted significant attention during the past decade in the conversion of sunlight to electricity because of their low cost and high efficiency.[1] In general, the DSSCs consist of a nanocrystalline metal oxide semiconductor film, dye sensitizer, redox electrolyte, and counter electrode. Among these parts, it has been acknowledged that the dye sensitizer is one of the key components for high power conversion efficiency. Therefore, many efforts have focused on the design and synthesis of the novel dyes, including Ru^{II},[2] Os^{III},[3] Fe^{II}[4] complexes, metal-free organic dyes,[5] and metalloporphyrins,[6] etc. Among them, the Ru^{II} complexes have been most intensively pursued as efficient sensitizers because they have an intense metal-to-ligand charge-transfer (MLCT) transition in the visible region, suitable ground- and excited-state redox properties, and good stability in the oxidized and reduced forms. The paradigms include $Ru(H_2dcbpy)_2(NCS)_2$ (H_2dcbpy = 2,2′-bipyridyl-4,4′-dicarboxylic acid) referred to as **N3**, a popular charge-transfer sensitizer in dye-sensitized solar cells,[7,8] and tris(thiocyanato)-2,2′,2′′-terpyridyl-4,4′,4′′-tricarboxylate ruthenium(II) complex (**black dye**) with visible absorption extending into the near-IR region up to 920 nm, producing an overall efficiency of 10.4%.[2a] In recent years many groups have designed and synthesized the heteroleptic ruthenium complexes of the type $Ru(H_2dcbpy)(L')(NCS)_2$ by means of changing the ancillary ligand (L′).[9] The carboxyl groups on H_2dcbpy in the complexes are responsible for the dye adsorption onto the semiconductor surface. The ancillary ligand L′ is not directly attached onto the semiconductor but can be used for tuning the overall properties of the complex. The function of the thiocyanato ligands is to tune the metal t_{2g} orbitals of ruthenium(II) and possibly to stabilize the hole that is being generated on the metal after having injected an electron into the conduction band of the metal oxide semiconductor.

Because of its excellent hole-transporting and donor properties, the carbazole group has attracted much interest in photoconductive,[10] photorefractive,[11] second-order nonlinear optical,[12a] solar energy conversion,[12b] and electroluminescent materials.[12c,12d,13a,b,e] However, carbazole-containing coordination compounds have been much less studied.[12c,12d,13,14] Our group has successfully incorporated carbazole into the Ru^{II} complexes for DNA binding and pH-induced emission switching/sensing studies,[13c,13d] and into Eu^{III}[13a,13b] and Re^{I}[13e] complexes for electroluminescent devices. Among the Ru^{II} complex-based photosensitizers developed for dye-sensitized solar cells, the incorporation of hole-conductors, such as triphenylamine and phenothiazine into the Ru^{II} complexes aimed at retarding interfacial charge-recombination dynamics and achieving

[a] College of Chemisty, Beijing Normal University,
Beijing 100875, China
Fax: +86-10-58802075
E-mail: kzwang@bnu.edu.cn

Supporting information for this article is available on the WWW under http://www.eurjic.org or from the author.

effective photoinduced charge separation, has received much interest,[9a,15a,15b] and significant contributions have been made by Meyer and coworkers,[15a] Durrant and coworkers,[9a] and Thelakkat and coworkers.[15b] To our surprise, however, the incorporation of the carbazole group, with similar functionalities to triphenylamine and phenothiazine, into the Ru^{II} complex-based solar cell dye sensitizers has received little attention,[15c,15d] prompting us to integrate the carbazole group into the Ru^{II} complex for DSSCs.[15c] On the other hand, the imidazole-containing ligands are poor π acceptors and good π donors, and also have the ability to control orbital energies, so electron- and energy-transfer processes by proton transfer[16] may produce interesting proton induced on-off emission switches for the complexes where the imidazole rings are coordinated or uncoordinated to the central metal ions.[16] Therefore, the imidazole group was also used to tune the ground- and excited-state properties of the Ru^{II} complex in this work.

In this study we report on a novel difunctional ruthenium complex $[Ru(Hecip)(Hdcbpy)(NCS)_2]^-\cdot[N(C_4H_9)_4]^+$ (where Hecip = 2-(9-ethyl-9*H*-carbazol-3-yl)-1*H*-imidazo[4,5-*f*][1,10]phenanthroline and Hdcbpy = monodeprotonated 2,2′-bipyridyl-4,4′-dicarboxylic acid) in which an ancillary ligand of Hecip contains not only the *N*-ethyl carbazole moiety but also uncoordinated imidazole rings. In a very recent note,[15c] we have reported four-step successive protonation/deprotonation processes of $[Ru(Hecip)(Hdcbpy)(NCS)_2]^-\cdot[N(C_4H_9)_4]^+$ in a Britton–Robinson buffer; however, one of the protonation/deprotonation processes that occurs over a very acidic pH region failed to fully resolve because of a solubility problem. In this paper, we extend the studies to the acid–base properties of $[Ru(Hecip)(Hdcbpy)(NCS)_2]^-\cdot[N(C_4H_9)_4]^+$ in a Britton–Robinson/DMF (v/v, 4:1) buffer solution, and to the application of this complex in DSSCs. We have observed five separate proton dissociations in the ground state, one of which occurs near the physiological pH region. One of the two observable excited-state protonation/deprotonation processes also occurs near the physiological pH region with emission off-on switching. This Ru^{II} complex-based DSSC was found to exhibit a higher open-circuit photovoltage albeit other somewhat poorer device parameters compared to those of the **N3** dye under the same experimental conditions. Here we would like to report these interesting observations.

Results and Discussion

Synthesis

The structure of the target complex $[Ru(Hecip)(Hdcbpy)(NCS)_2]^-\cdot[N(C_4H_9)_4]^+$ is shown in Scheme 1. The synthetic strategy adopted for the preparation of the complex is outlined in Scheme S1.[15c] The synthetic method was reported in our previous note,[15c] and is similar to a literature method,[9a,17] but we omitted the procedure of separating the intermediate $[Ru(Hecip)(H_2dcbpy)Cl_2]$. The final product $[Ru(Hecip)(Hdcbpy)(NCS)_2]^-\cdot[N(C_4H_9)_4]^+\cdot CH_3OH\cdot 3H_2O$, which is abbreviated as **Ru(Hecip)** hereafter for simplicity, was fully characterized by UV/Vis and emission spectroscopy, which will be addressed below, ^1H NMR spectroscopy, elemental analysis, and matrix assisted laser desorption ionization and time-of-flight (MALDI-TOF) mass spectrometry. The ^1H NMR spectrum of **Ru(Hecip)** and the assignments of the proton resonance signals are shown in Figure S1.

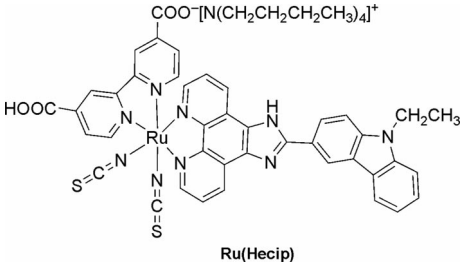

Scheme 1. The structure of **Ru(Hecip)**.

Electronic Absorption Spectra

The electronic absorption spectra of Hecip, **Ru(Hecip)**, and **N3** in ethanol are compared in Figure 1. The data are summarized in Table 1. The absorption spectrum of **Ru(Hecip)** shows four bands centered at ca. 530, ca. 342 (shoulder), ca. 310 (shoulder), and ca. 300 nm. By comparing the spectrum with those for Hecip and $dcbpy^{2-}$, the two bands at 342 and 300 nm are assigned to a π–π* transition localized on Hecip. A shoulder at ca. 310 nm is attributed to a π–π* transition localized on Hdcbpy. The broad absorption band at 530 nm is assigned to the MLCT (metal-to-ligand charge-transfer) transition, as for other heteroleptic ruthenium complexes,[18,19] and is blue shifted by 9 nm compared to a peak at 539 nm for the homoleptic complex **N3**.[20a] The blue shift is probably as a result of the higher lying LUMO energy of Hecip than that of H_2dcbpy. It is noteworthy from Figure 1 that **Ru(Hecip)** has greater molar extinction coefficients, except for slightly lower ones over the spectral region of 530–700 nm, compared to **N3**.

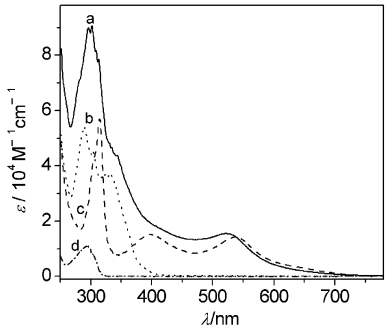

Figure 1. UV/Vis absorption spectra of **Ru(Hecip)** (a), Hecip (b), **N3** (c), and $dcbpy^{2-}$ (d) in ethanol solutions with concentrations of ca. 1.5×10^{-5} M.

Table 1. Electronic absorption, photophysical, and electrochemical data.[a]

Compound	Absorption maxima [nm][b] (ε /10^4 $M^{-1}cm^{-1}$)			Emission, λ_{max} /nm (Φ)	$E_{1/2}^{Ox}$ /V	$E_{1/2}^{Red}$ /V	
	$\pi \rightarrow \pi^*$(Hecip)	$\pi \rightarrow \pi^*$($H_i$dcbpy) (i = 0 or 1 or 2)	$d\pi \rightarrow \pi^*$(MLCT)		$Ru^{III/II}$	Hecip	[$H_i$dcbpy] (i = 1 or 2)
Hecip	291 (5.24), 330 (3.71)			472 (0.019)		–2.32	
Na_2dcbpy		294 (1.12)					
Ru(Hecip)	300 (9.01), 342 (4.14)	309 (8.13)	530 (1.52)	780 (0.0009)	0.76	–2.18	–1.74[c]
N3[20a,29]		314 (4.82)	398 (1.40), 539 (1.42)	797 (0.0004)	0.85		–1.95

[a] The electrochemical data were reported vs. SCE. [b] The data were measured in ethanol. [c] An anodic peak potential.

The visible absorption spectra for **Ru(Hecip)** adsorbed on the TiO_2 substrate, and for **Ru(Hecip)** dissolved in ethanol, which have been normalized at their maximum peaks, are compared in Figure S2. The maximum absorption peak positions are strongly affected by the adsorption, blue shifting to 503 nm from 525 nm when the complex is attached to the TiO_2 surface. The blue shift of 22 nm is much more evident than a slight blue shift reported for **N3**,[20b] indicating a strong electron coupling between **Ru(Hecip)** and the TiO_2. The blue shifts can be explained by (i) the decrease in the electronic charge on the dye by the electron acceptor character of the TiO_2, and (ii) the stabilization of the HOMO level of the dye caused by electronic delocalization through the titanates at the TiO_2-dye interface.[20c]

Acid–Base Equilibria in the Ground and Excited States

UV/Vis Spectra and the Ground-State pK_a

To further investigate the protonation/deprotonation processes of **Ru(Hecip)** over a pH range of <2.0,[15c] 20% DMF was added to a Britton–Robinson buffer in order to enhance the solubility of **Ru(Hecip)** over this pH range. The changes in the UV/Vis spectra of the complex in a Britton–Robinson/DMF (v/v, 4:1) buffer solution as a function of pH (0.22–13.0) are shown in Figure 2. It is clear from Figure 2 that the complex underwent five successive deprotonation processes upon raising the pH from 0.22 to 13.00. As shown in Figure 2 (a), an increase in pH from 0.22 to 2.03 leads to an obvious increase in absorption intensities for the band at 314 nm along with a 6-nm blue shift, and an evident decrease in the intensities of the shoulder at 375 nm. The first step deprotonation is assigned to the dissociation of one proton on the carboxyl group of the H_2dcbpy moiety. A further increase in pH from 2.13 to 3.20 results in the second-step spectral changes where the absorption intensities for the shoulder at 350 nm are a little increased, and the intensities for the band at 307 nm are decreased. The spectral changes observed above are assigned to the dissociation of the proton on the carboxyl group of the Hdcbpy moiety. The next deprotonation step took place over a pH of 3.00–5.00, and is assignable to the dissociation of the one proton on the protonated imidazole ring, resulting in significantly increased absorption intensities of the bands at 300 and 345 nm, and a decrease in the MLCT band at 535 nm with a 25-nm blue shift. Upon further increasing the pH from 5.00 to 7.20 the deprotonation process, which deals with the proton dissociation of the protonated *N*-ethyl carbazole moiety, occurred accompanied by the following spectral features: the intensities of the bands at 300 and 345 nm increased with the absorption intensities. As the pH increased from 8.00 to 13.00 the deprotonation of the neutral imidazole ring occurred and was characterized by evident increases in the intensities of the bands at 300 and 342 nm. The acidity ionization constants of **Ru(Hecip)** could be derived based on the spectral changes discussed above. By nonlinear sigmoidal fits of the data in the insets of Figure 2, the other five ground-state acidity

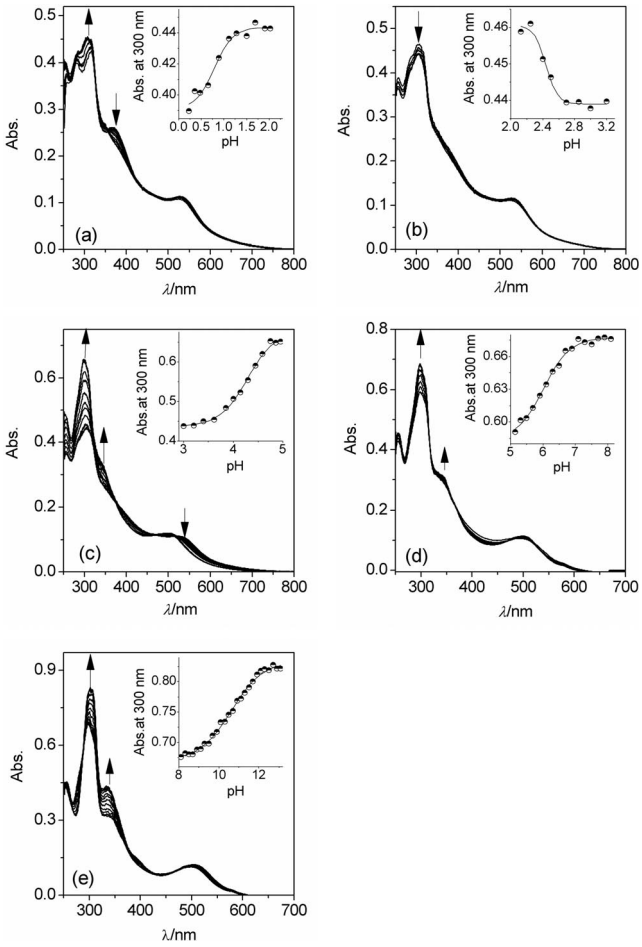

Figure 2. The changes in UV/Vis spectra of the complex **Ru(Hecip)** in a Britton–Robinson/DMF (v/v, 4:1) buffer solution upon raising the pH: pH = 0.22–2.00 (a), pH = 2.12–3.00 (b), pH = 3.00–5.00 (c), pH = 5.00–7.00 (d), and pH = 8.00–13.00 (e). The insets show the plots of absorbances at 300 nm versus pH.

ionization constants of $pK_{a1} = 0.79 \pm 0.07$, $pK_{a2} = 2.44 \pm 0.02$, $pK_{a3} = 4.29 \pm 0.03$, $pK_{a4} = 6.02 \pm 0.06$, and $pK_{a5} = 10.63 \pm 0.05$ were obtained. A comparison of the pK_a values for **Ru(Hecip)** with those for H_2dcbpy-containing or analogue Hecip Ru^{II} complexes are listed in Table 2. The pK_{a1} value, which is observable in a Britton–Robinson/DMF buffer in the current study, was unobservable in our previous study in a Britton–Robinson aqueous buffer.[15c] The other four pK_a values are similar to those we previously reported in the Britton–Robinson aqueous buffer.[15c] As addressed above, we have observed two-step proton dissociation processes of the carboxyl acids on **Ru(Hecip)** with $pK_{a1} = 0.79$ and $pK_{a2} = 2.44$. These two pK_a values are similar to the values of $pK_{a1} < 0.5$ and $pK_{a2} = 2.65$ observed for $[Ru(bpy)_2(H_2dcbpy)]^{2+}$ by Shimidzu et al.,[21] and $pK_{a1} = 1.75$ and $pK_{a2} = 2.85$ derived for the same complex by Nazeeruddin and Kalyanasundaram,[22] as well as $pK_{a1} = 1.4$ and $pK_{a2} = 2.2$ reported by Nazeeruddin et al. for the proton dissociation of two carboxyl groups of H_2dcbpy on [Ru(dmbip)(dcbpy)(H_2O)] [dmbip = 2,6-bis(1-methylbenzimidazol-2-yl)pyridine].[23] The $pK_{a3} = 4.29$ value, observed for the proton dissociation of the protonated imidazole moiety of Hecip on the complex, is 0.13 pH units higher than a pK_a value of 4.16 reported for a similar proton disso-

Table 2. The comparison of ground- and excited-state acidity ionization constants for **Ru(Hecip)** with those reported for representative related Ru^{II} complexes.[a]

Complexes	pK_{ai}	pK_{ai}*	Ref.
$[Ru(H_2dcbpy)(bpy)_2]^{2+}$	<0.5, 2.7	3.4, 4.5	[21]
$[Ru(H_2dcbpy)(bpy)_2]^{2+}$	1.75, 2.85	4.25	[22]
[Ru(dcbpy)(dmbip)(H_2O)]	1.4, 2.2, 11.4		[23]
[Ru(H_2dcbpy)(dmbip)(CN)]		2.5, 4.5	[23]
$[(bpy)_2Ru(ebipcH_2)Ru(bpy)_2]^{4+}$	4.16, 5.17, 9.65, 12.09	4.54, 5.07, 9.76, 12.09	[13c]
Ru(Hecip)	<2.00, 2.67, 4.61, 5.82, 11.58[b]	–, –, –, 7.83, 11.19	[15c] [b]
Ru(Hecip)	0.79, 2.44, 4.29, 6.02, 10.63[c]	–, –, –, 8.09, 9.47	this work[c]

[a] H_2dcbpy = 2,2′-bipyridyl-4,4′-dicarboxylic acid; dmbip = 2,6-bis(1-methylbenzimidazol-2-yl)pyridine; ebipcH_2 = *N*-ethyl-4,7-bis([1,10]-phenanthroline[5,6-*f*]imidazol-2-yl)carbazole. [b] Measured in a Britton–Robinson buffer. [c] Britton–Robinson/DMF (v/v, 4:1).

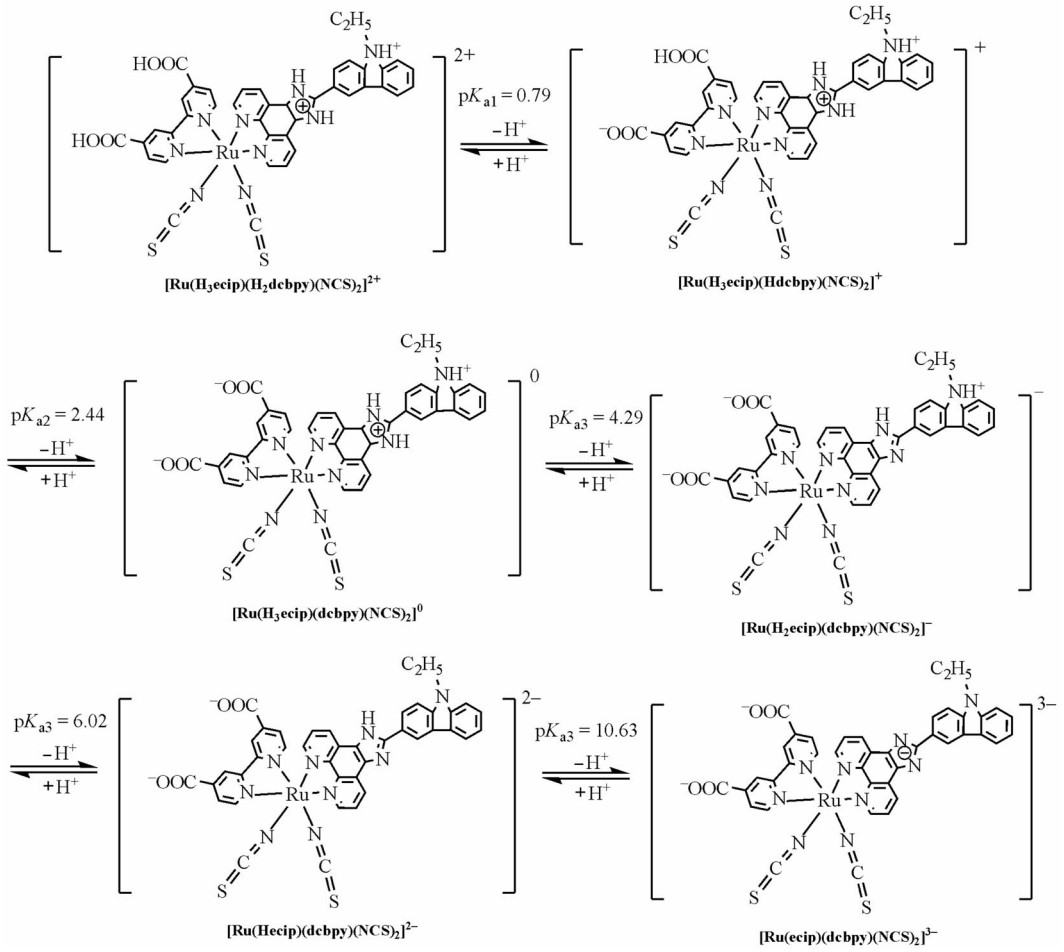

Scheme 2. The ground-state acid–base reactions of **Ru(Hecip)** in a Britton–Robinson/DMF (v/v, 4:1) buffer solution.

ciation of H_2ebipc on $[(bpy)_2Ru(H_2ebipc)Ru(bpy)_2]^{4+}$ {H_2ebipc = *N*-ethyl-4,7-bis([1,10]-phenanthroline[5,6-*f*]-imidazol-2-yl)carbazole}.[13c] A pK_{a4} = 6.02 value, derived for the proton dissociation of the protonated *N*-ethyl carbazole moiety of Hecip on the complex, is consistent with H_2ebipc on $[(bpy)_2Ru(H_2ebipc)Ru(bpy)_2]^{4+}$.[13c] A p$K_{a5}$ = 10.63 value, derived for the proton dissociation of the neutral imidazole ring of Hecip on the complex, is 1.46 pK_a units less than the corresponding proton dissociation of H_2ebipc on $[(bpy)_2Ru(H_2ebipc)Ru(bpy)_2]^{4+}$.[13c] It is noteworthy that the protonation/deprotonation reaction for the *N*-ethyl carbazole group on the complex occurs near the physiological pH region (pH 5.0–7.0), giving interesting hints for applications of the complex in bioinorganic chemistry and medicine. Our laboratory is currently exploring these possibilities. On the basis of the above analyses, we have summarized protonation/deprotonation processes in a Britton–Robinson/DMF (v/v, 4:1) buffer of **Ru(Hecip)** in Scheme 2.

*Emission Spectra and the Excited-State pK_a**

Spectrofluorimetric pH titrations were also carried out in a Britton–Robinson/DMF (v/v, 4:1) buffer at 298 K. The emission spectral changes of **Ru(Hecip)** as a function of pH in the buffer and at an excitation of λ_{ex} = 530 nm are shown in Figure 3, and the changes in emission quantum yields versus pH are displayed in the insets. The emission quantum yields were calculated by comparison with $[Ru(bpy)_3]^{2+}$ (ϕ = 0.033)[24] in an aerated aqueous solution at room temperature using Equation (1)

$$\phi = \phi_{std}(A_{std}/A)(I/I_{std}) \quad (1)$$

where ϕ and ϕ_{std} are the quantum yields of the unknown and standard samples; A and A_{std} are the absorbances at the excitation wavelength; I and I_{std} are the integrated emission intensities.

The increases in pH from 0.22 to 3.0 almost unaltered the emission spectra of **Ru(Hecip)**, which showed dual emission with a very weak band centered at 645 nm, and a dominant one centered at 780 nm. In the case of a mixed ligand complex the MLCT excited state should in principle be located on any of the ligands; however, in fluid solutions the reports on dual emission of Ru^{II} complexes are rare.[25e–25k]This is probably because the two emissive states are usually separated by a small energy barrier that is not large enough to prevent interconversion of populations or the luminescence properties are insufficiently different in energy.[25e] Tor and coworkers[25e,25f] reported dual emission from mononuclear and dinuclear Ru^{II} complexes containing alkyne-substituted phen ligands, and they assigned the dual emission from two spatially separated MLCT excited states with one localized on the extended 1,10-phenanthroline (resulting in the lower energy emission) and the other on the bipyridine coligands (correlated to the higher energy emission).[25e] On the basis of the above discussions, we assigned the higher energy emissions at 645 nm (λ_{ex} = 530 nm, Figure 3, a) of pH 1.0–3.5 **Ru(Hecip)** aqueous solutions to the Ru→dcbpy charge-transfer excited state, and the lower energy emission at 780 nm to the Ru→Hecip charge-transfer excited state. Since a dual emission was observed at 660 nm and 780 nm for **Ru(Hecip)**, we recorded pH effects on the excitation spectra at the emission wavelengths of 780 nm (see Figure S3) and 660 nm (see Figure S4). Excitation spectra obtained at both emission maxima are similar with the visible light maximum excitation centered at 470 nm, suggesting that both emissions are based on MLCT emissions, similar to the behavior of the dually emissive $[Ru(bpy)_2(pztr)]PF_6$, (Hpztr = 3-(pyrazin-2-yl)-1,2,4-triazole).[25g] Interestingly, the dual emission we reported here was observed in the Britton–Robinson/DMF (v/v, 4:1) buffer solution, but was not observed in the Britton–Robinson aqueous buffer.[15c] At 470 nm, **Ru(Hecip)** in the Britton–Robinson/DMF (v/v, 4:1) buffer solution showed interesting on-off-on-off emission switching as the pH increased from 0.3 to 11.0 with dominant bands centered at (Figure S5) 660 nm and an ill-defined shoulder band located on the lower energy side. That is to say, the dual emission of **Ru(Hecip)** is solvent[25l] and excitation wavelength dependent, and its excitation spectra are different from its absorption spectrum, which are similar to the behaviors reported for dually emissive $[Ru(bpy)(HDPA)_2]^{2+}$ (HDPA = 2,2′-dipyridylamine).[25j,25k]

In order to derive the excited-state properties, it is necessary to obtain well-defined emission bands at the lower energy side (780 nm). Accordingly in the following we shall concentrate our discussions on 530-nm excited emission

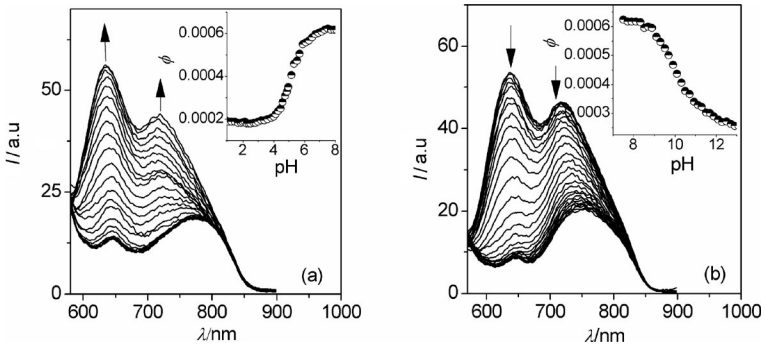

Figure 3. The changes in emission spectra (λ_{ex} = 530 nm) of **Ru(Hecip)** in a Britton–Robinson/DMF (v/v, 4:1) buffer solution upon raising the pH: pH = 3.00–7.00 (a), and 8.00–13.00 (b). The insets show the plots of emission quantum yields versus pH.

properties of **Ru(Hecip)** in the Britton–Robinson/DMF (v/v, 4:1) buffer solution. Upon increasing the pH from 3.5 to 7.0, the intensities of the emission bands at 645 and 675 nm (Figure 3, a; λ_{ex} = 530 nm) were both enhanced, but finally the former higher-energy band at 645 nm became stronger with a blue shift of 9 nm, while the latter lower-energy band at 775 nm became weaker with a large blue shift of 57 nm (Figure 3, a). Since occurring over a pH range that is almost the same as that for the ground-state deprotonation reaction of the protonated *N*-ethyl carbazole moiety on the complex, as observed from a UV/Vis spectrophotometric titration, the above spectral changes are assigned to the excited-state deprotonation reaction of the same proton. Upon inspection of the changes in emission quantum yields versus pH (inset of Figure 3, a), the complex acted as a physiological-pH-responsive emission switch with an emission enhancement factor of ca. 3.3 based on emission quantum yields. To the best of our knowledge, physiological-pH responsive metal complexes are very rare.[25a] Upon further increasing the pH from 8.00 to 13.00 the intensities of the emission bands at 636 and 720 nm both decreased, but finally the former band became weaker with a red shift of 9 nm, while the latter band became stronger with a large red shift of 30 nm (Figure 3, b). The spectral changes described above are attributed to the excited state deprotonation of the imidazole moiety on the complex. The plots of emission quantum yields at λ = 750 nm versus pH (see insets a and b in Figure 3) show two reverse profiles corresponding to two independent excited-state protonation/deprotonation processes as mentioned above, in contrast to the five-step ground-state protonation/deprotonation reactions observed by UV/Vis spectrophotometric titrations, indicating that the other three excited-state deprotonation processes did not cause observable emission spectral changes as the excitation wavelength was set at 530 nm in the spectrofluorimetric titrations. A luminescence off–on–off switching action was achieved by the combined deprotonation processes of protonated *N*-ethyl carbazole and imidazole moieties on the complex. pH-Induced luminescence on–off or off–on switches could be used to mimic many life processes, such as the functions and activities of "switch on" or "switch off" enzymes within a narrow pH window.[25a–25d] The excited-state acidity ionization constant, pK_a*, could be roughly determined on the basis of the Förster cycle,[26a] which thermodynamically correlates the pK_a* with the pK_a value by Equation (2), where T is the temperature (298 K), and ν_B and ν_{HB} denote the wavenumber (cm^{-1}) of the deprotonated and the protonated forms, respectively. In practice ν_B and ν_{HB} are often difficult or even impossible to obtain. A good approximation is to use the emission maxima for ν_B and ν_{HB} since a protonation equilibrium is almost certainly established between the ^{3}MLCT states.[26b] Therefore, the energies of the emission maxima in wavenumbers were used in Equation (2), and two pK_a* values of pK_{a4}* = 8.09 ± 0.03 and pK_{a5}* = 9.47 ± 0.03 were obtained. The excited-state pK_{a4}* value is 1 pK_a unit greater than the ground-state pK_{a4}, suggesting that the electron density in the excited state of [Ru(H_2ecip)(dcbpy)$(NCS)_2$]$^-$* is significantly higher than in the ground state, and that the excited electron is mainly delocalized on H_2ecip^+ rather than dcbpy. If the excited electron of Ru(H_2ecip)(dcbpy)$(NCS)_2$]$^-$* was delocalized on dcbpy, which was fully deprotonated, it would not result in a big increase in electron densities on H_2ecip in Ru(H_2ecip)-(dcbpy)$(NCS)_2$]$^-$*, and accordingly no remarkable changes between the excited-state pK_{a4}* and ground-state pK_a of the proton on H_2ecip of Ru(H_2ecip)(dcbpy)$(NCS)_2$]$^-$* would be observed. However, the pK_{a5}* value is less than the pK_{a5} value, indicating that the electron in the excited-state of [Ru(Hecip)(dcbpy)$(NCS)_2$]$^{2-}$* is mainly populated on dcbpy rather than Hecip, similarly to [Ru(dmbip)(dcbpy)(CN)][23] with the excited-state electron located on dcbpy rather than dmbip. Namely, the deprotonation of the protonated *N*-ethyl carbazole moiety of the complex switches the MLCT route from a mainly $Ru^{II} \rightarrow H_2$ecip to a mainly $Ru^{II} \rightarrow$ dcbpy charge transfer in nature, and switches the luminescence "on" near the physiological pH region.

$$pK_a^* = pK_a + (0.625/T)(\nu_B - \nu_{HB}) \quad (2)$$

FTIR Spectra

IR spectroscopy is a powerful tool for investigating the binding modes of the carboxylate group of Ru^{II} dyes to TiO_2 nanocrystalline films.[27] The binding modes have been a hot topic because they play a key role in the stability and the charge injection efficiency of the solar cells. The following four kinds of binding modes have been put forward for chemisorption: unidentate linkage (the formation of an ester-type bond) via chemical bond formation of Ti with an hydroxy oxygen atom, bidentate linkage with the two oxygen atoms of the COO^- group equally interacting (chelating) with Ti, bridging linkage with each of two oxygen atoms of COO^- equally bonding to one different Ti, and pseudobridging linkage with one of two Ti atom in the bridging linkage being replaced by hydrogen atoms of a water molecule. An empirical rule based on the frequency difference $\Delta\nu$ between COO^- antisymmetric and symmetric stretches for the assessment of the binding modes has been proposed.[7a,27b,d,g] If $\Delta\nu$ for the adsorbed film is less than that for the free state, the binding mode is either bidentate chelate or bridging. While if $\Delta\nu$ for the adsorbed film is greater than or equal to that of the free state, the binding mode is unidentate. The IR spectrum of **Ru(Hecip)** recorded from KBr pellets is compared with that adsorbed on the TiO_2 film in Figure 4. In the present study, a $\Delta\nu$ value of 238 cm^{-1} was observed for the KBr pellet [ν_{asym} (COO^-) = 1602 cm^{-1} and ν_{sym} (COO^-) = 1364 cm^{-1}] and a value of 219 cm^{-1} was found for the film [ν_{asym} (COO^-) = 1601 cm^{-1} and ν_{sym} (COO^-) = 1382 cm^{-1}], indicative of bridging or bidentate coordination of the carboxylate group on the TiO_2 surface. This conclusion is consistent with those reported for $(Bu_4N)_2$[Ru(H_2dcbpy)$_2(NCS)_2$] (**N719**)[27b] and other analogue Ru^{II} complexes.[7,27a,e–g] By using the bipyridine ν(C=C) at 1542 cm^{-1} as an internal standard, the vi-

bration modes of ν(C–O) for nonequivalent oxygen at 1234 cm^{-1} for the KBr pellet was observed to be attenuated in intensity as the complex was anchored to the film, while the intensities in the equivalent oxygen $\nu_{as}(COO^-)$ and $\nu_s(COO^-)$ vibrations for the absorbed film become dominantly strong compared to those observed in the KBr pellet, also supporting a bridging or bidentate anchoring mode of the Ru^{II} complex on the TiO_2 surface.[27b] The other important features include the following: (i) the intensity of the band at ca. 1472 cm^{-1} attributed to the $\delta(CH_2)$ of Bu_4N^+ cation[7] in the film is greatly decreased relative to that in the KBr pellet due to the fact that the counter cation of Bu_4N^+ was left in the solution and was washed away as the Ru^{II} complex was anchored to the TiO_2 surface; (ii) the KBr pellet shows a strong peak at 2102 cm^{-1} from the *N*-coordinated thiocyanate ν(NC) vibration,[27a] which is close to 2105 cm^{-1} observed for **N719**,[7] and is shifted to a lower energy compared to 2123 cm^{-1} observed for **N3**,[7] and appears as a broader, weaker and red-shifted band at ca. 2097 cm^{-1} for the adsorbed film; and (iii) a peak at 1712 cm^{-1}, observed for the KBr pellet from the ν(C=O) vibration of the protonated carboxyl group, disappeared in the film, supporting the fact that deprotonation of the carboxylic group took place at the TiO_2 surface. All the evidences mentioned above support a bridging or bidentate anchoring mode,[27b,27g] rather than the formation of an ester bond.[27c,27d]

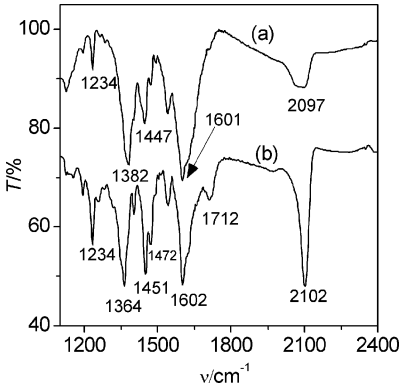

Figure 4. FTIR spectra of **Ru(Hecip)** in absorbed film on TiO_2 (a) and in a KBr pellet (b).

Electrochemistry

A cyclic voltammogram of **Ru(Hecip)** in DMF is shown in Figure 5, and the electrochemical data are collected in Table 1. The complex displays one reversible wave at $E_{1/2}$ = +0.76 V vs. SCE attributable to the $Ru^{III/II}$ redox couple,[28] a quasi-reversible couple at $E_{1/2}$ = –2.18 V vs. SCE assigned to the $Hecip^{0/-1}$ redox couple, and an irreversible anodic wave at –1.74 V vs. SCE that is assigned to the Hdcbpy-based reduction process.[29] As far as the $Ru^{III/II}$ redox waves are concerned, the dependence of the anodic peak currents on the square root of the scanning rates is characteristic of a diffusion-controlled redox process. The $Ru^{III/II}$ $E_{1/2}$ value observed for **Ru(Hecip)** is less positive by 0.1 V than the value for **N3**, most likely because Hecip is a stronger electron donor than Hdcbpy. It is noteworthy that the excited state oxidation potential ($E_{1/2}$* $Ru^{III/II}$ = $E_{1/2}$ $Ru^{III/II}$ – E^{00}) of **Ru(Hecip)** is derived to be –0.94 V vs. SCE on the basis of an E^{00} value of 1.69 eV calculated from a visible absorption edge of 730 nm and an $E_{1/2}$ $Ru^{III/II}$ value of +0.75 V vs. SCE, indicating a sufficient driving force to allow for electron injection from the excited **Ru(Hecip)** to the conduction band of TiO_2, since the flat band potential of TiO_2 is known to be near –0.70 V vs. SCE.[1f,20c]

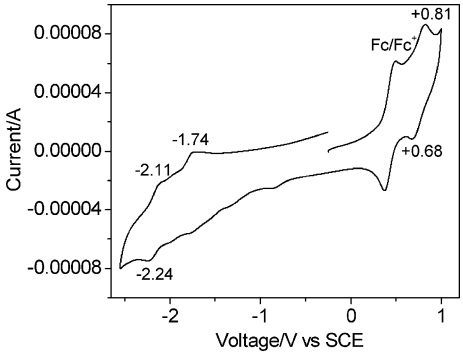

Figure 5. Cyclic voltammogram of **Ru(Hecip)** in DMF (1.40 mM) at a scan rate of 500 $mV\,s^{-1}$.

Photovoltaic Performance

The incident monochromatic photon-to-current conversion efficiency (IPCE) and the overall light-to-electric power conversion efficiency of the solar cells are evaluated according to Equations (3) and (4), respectively,

$$\mathrm{IPCE}(\%) = \frac{1240 \times I_{SC}}{\lambda \times \phi} \times 100 \quad (3)$$

$$\eta = \frac{ff \times V_{oc} \times I_{sc}}{\phi} \quad (4)$$

where I_{sc} is the short-circuit photocurrent ($mA\,cm^{-2}$), V_{oc} is the open circuit voltage, *ff* is the fill factor of the cell, ϕ is the incident irradiative flux ($mW\,cm^{-2}$), and λ is the incident light wavelength (nm).

The current-voltage characteristic curves and the plots of IPCE versus the excitation wavelength for solar cells sensitized with **Ru(Hecip)** and **N3** are shown in Figures 6 and 7, respectively. The device parameters for **Ru(Hecip)** and **N3** sensitized solar cells are compared in Table 3. From Figure 6, the short-circuit photocurrent density (I_{sc}), open-circuit voltage (V_{oc}), and fill factor (*ff*) of the **Ru(Hecip)**-based solar cell were found to be 7.8 $mA\,cm^{-2}$, 356 mV, and 51%, respectively, corresponding to an overall conversion efficiency (η) of 1.5%, derived from Equation (4). The open-circuit potential of 356 mV observed for the **Ru(Hecip)**-sensitized solar cell is higher than a value of 310 mV for an **N3**-based device, which may be mainly caused by the fact that the number of protons in the former case, one, is less

than a much greater number of four for the latter case. It was reported that the open-circuit photovoltage of DSSCs depends on the Fermi level of TiO_2.[31] Generally, if the proton concentration on the TiO_2 surface becomes lower, and the Fermi level of the nanocrystalline TiO_2 becomes higher then the V_{oc} is higher due to the increase in the gap between the redox couple iodide/triiodide and the Fermi level, e.g. an open-circuit potential of 730 mV was reported for the two proton-containing **N719**, but 600 mV for the four proton-containing **N3**.[7] The short-circuit photocurrent density of 7.80 mA cm^{-2} for the **Ru(Hecip)**-based device is 1.24-fold lower than that (17.5 mA cm^{-2}) observed for the **N3** dye-based device. Also, an IPCE peak value of 63% as shown in Figure 7, and an overall light-to-electric power conversion efficiency η of 1.5% derived for the **Ru(Hecip)**-based device, are less than the corresponding values of 75% and 2.3% observed for the **N3**-based device. In order to clarify which factors contribute to the lower IPCE value observed for the **Ru(Hecip)**-based device we will consider Equation (5).

$$IPCE(\lambda) = LHE(\lambda) \times \varphi_{inj} \times \eta_c \quad (5)$$

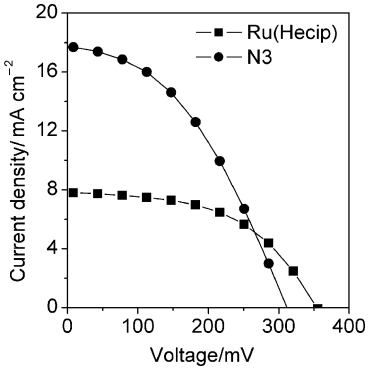

Figure 6. The photocurrent-voltage characteristics of **Ru(Hecip)** and **N3**-sensitized TiO_2 nanocrystalline solar cells.

The IPCE is expressed as the product of the light harvesting efficiency [LHE(λ)] of the photoelectrode at wavelength λ, the quantum yield for electron injection (ϕ_{inj}) from the excited sensitizer to the conduction band of TiO_2, and the efficiency of collecting the injected electron (η_c) at the conducting glass substrate. The LHE at the maximum absorption wavelength can be estimated according to Equation (6)[32]

$$LHE = 1 - 10^{-\Gamma\sigma} \quad (6)$$

where Γ is the surface coverage in units of mol cm^{-2} of the dye molecules on TiO_2 and σ is the absorption cross section in units of cm^2 mol^{-1} obtained from the extinction coefficient of the dye by multiplication with 1000 cm^3 L^{-1}.

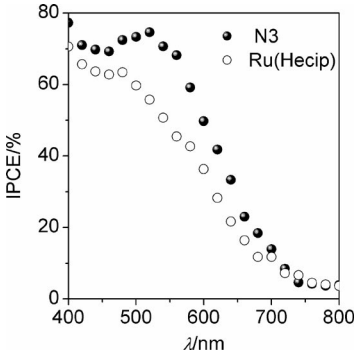

Figure 7. The plots of IPCE values vsersus excitation wavelengths for **Ru(Hecip)** and **N3**-sensitized TiO_2 nanocrystalline solar cells. Mediator: I_2 (0.05 M) and LiI (0.5 M) in 50% acetonitrile + 50% PC.

The optical cross sections σ near the absorption maximum of the dyes were estimated to be 1.52×10^7 cm^2 mol^{-1} for **Ru(Hecip)** and 1.42×10^7 cm^2 mol^{-1} for **N3** by using the molar extinction values in the ethanol solutions. The surface coverage values of 1.10×10^{-7} mol cm^{-2} for **Ru(Hecip)** and 4.70×10^{-7} mol cm^{-2} for **N3** were obtained by desorbing the complex from the TiO_2 film into a 0.02 M KOH/methanol (v/v, 1:1) solution, and measuring the absorption spectra of the resultant solutions. Thus, the light harvesting efficiency (LHE) at the maximum absorption wavelength was estimated to be 98% for **Ru(Hecip)** and ca. 100% for **N3** at the absorption maxima. The LHE values were derived to be 0.98 and ca. 1.0 for the **Ru(Hecip)**- and **N3**-coated ITO electrodes, respectively, indicating that both **Ru(Hecip)** and **N3** could efficiently capture photos as the sensitizers of the dye-sensitized solar cells with the peak LHE values are close to each other. Thus the lower electron injection quantum yield of **Ru(Hecip)** made a contribution to the lower IPCE value, and accordingly to the lower short-circuit photocurrent observed for the **Ru(Hecip)**-based device compared to the **N3**-based device. One of the factors affecting the electron injection quantum yield is that the lower proton concentration on the interface of TiO_2 and the electrolyte for the **Ru(Hecip)**-based device than that of

Table 3. The device parameters for **Ru(Hecip)**- and **N3**-sensitized TiO_2 nanocrystalline solar cells.

Dyes	V_{oc} /mV	I_{sc} /mA cm^{-2}	*ff* (%)	η (%)	IPCE$_{max}$ (%)	Ref.
Ru(Hecip)	356	7.8	51	1.5	63	this work[a]
N3	310	17.5	44	2.3	74	this work
N3	686	11.1	72	5.5	/	[30] [b]
N3	580	1.26	62	4.54	40	[9c] [c]
N3	600	19.0	65	7.4	85	[7] [d]

[a] Measured in I_2 (0.05 M), LiI (0.5 M) in 50% acetonitrile and 50% PC. [b] 1-Propyl-3-methylimidazolium iodide (0.6 M), I_2 (0.05 M), LiI (0.05 M), and *tert*-butylpyridine in 3-methoxypropionitrile (0.5 M). [c] Tetrabutylammonium iodide (0.5 M), LiI (0.02 M), I_2 (0.05 M), and 4-*tert*-butylpyridine (0.5 M) that was dissolved in acetonitrile. [d] Dimethylpropylimidazolium iodide (0.6 M) and I_2 in methoxyacetonitrile (0.05 M).

the **N3**-based device results in raising the TiO_2 conduction band as mentioned above, affording unfavorable energetics of electron injection.[7] Experiments are being planned that will explore other reasons affecting the electron injection quantum yield and charge-transfer dynamics of the dye-sensitized nanocrystalline TiO_2 films in the near future.

Conclusions

A new heteroleptic ruthenium complex containing a carbazole-functionalized 1,10-phenanthroline ligand, **Ru(Hecip)**, has been synthesized and well characterized. The Ru^{II} complex, in a Britton–Robinson/DMF (v/v, 4:1) buffer solution, was found to exhibit dual emission via two different MLCT processes (Ru→Hecip and Ru→Hdcbpy), and five separated protonation/deprotonation steps in the ground state, and two/three observable protonation/deprotonation steps in the excited state, with one of the protonation/deprotonation processes in both the ground state and excited state occurring near the physiological pH region. The complex was shown to act as off-on-off/on-off-on-off-type emission switches when excited at 530 nm/470 nm, and as a strong binder to the TiO_2 surface via a bridging or bidentate anchoring mode. A **Ru(Hecip)**-sensitized TiO_2 nanocrystalline solar cell showed a higher open-circuit voltage, but is less efficient than **N3** in view of both a maximum IPCE value of >60% and a power efficiency of 1.5% under simulated sunlight at the irradiation of 100 mW cm^{-2}.

Experimental Section

Materials and Reagents: DMF and absolute ethanol were refluxed over CaH_2, and Mg and I_2, respectively, and were subsequently distilled prior to use. All other solvents were obtained from commercial sources and used as received. Sephadex LH-20 was purchased from Pharmacia (Sweden). The substrates of fluorine-doped tin oxide (FTO) with a sheet resistance of 30 Ω sq^{-1} on glass were provided by the General Research Institute for Nonferrous Metals (China), and were each rinsed successively with a basic isopropyl alcohol solution, ethanol, and acetone under supersonication for 10 min prior to use.[31] $RuCl_3 \cdot 3H_2O$ was purchased from Acros. 2,2′-Bipyridyl-4,4′-dicarboxylic acid (H_2dcbpy),[33] 2-(9-ethyl-9*H*-carbazol-3-yl)-1*H*-imidazo[4,5-*f*][1,10]phenanthroline (Hecip),[13b,13e] dichlorotetrakis (dimethylsulfoxide) ruthenium(II) [$Ru(DMSO)_4Cl_2$],[34] and $Ru(H_2dcbpy)_2(NCS)_2$ called **N3** dye,[35] were synthesized by literature methods. **Ru(Hecip)** was synthesized as described previously,[15c] and the synthetic details are given in the Supporting Information.

Analytical Measurements: UV/Vis absorption and emission spectra were recorded in a 1 cm path length quartz cell with a GBC Cintra 10e UV/Vis spectrophotometer and a Shimadzu RF-5301PC spectrofluorimeter, respectively. The FTIR spectra were obtained using a Nicolet Avtar 360 FT-IR spectrometer with a 2 cm^{-1} resolution. For the IR spectra of the complex anchored onto TiO_2 films, complex/TiO_2 powder scratched off the glass substrate was pressed into KBr pellets. ^{1}H NMR spectra were measured with a Bruker DRX-500 NMR spectrometer with [D_6]DMSO as the solvent at room temperature. The reported chemical shifts were in ppm against TMS. Elemental analyses (C, H, and N) were carried out with a Vario EL elemental analyzer. Matrix assisted laser desorption ionization and time-of-flight (MALDI-TOF) mass spectra were collected with an API Q-star pulsar I/OMALDI/QQ-TOF mass spectrometer. The cyclic voltammogram of **Ru(Hecip)** in DMF containing (n-$C_4H_9)_4NPF_6$ (0.1 M) was obtained with a CHI-601 electrochemical system, using glass carbon as a working electrode, a silver wire as a quasi-reference electrode, and a Pt wire as an auxiliary electrode. Ferrocene was added at the end of each experiment to serve as the internal reference. Its half-wave potential $E_{1/2}{}^0$ [$E_{1/2}{}^0 = 0.5 \times (E_{pa} + E_{pc})$] was taken to be +0.425 V vs. SCE.[36]

Acid–Base Equilibria: The ground- and excited-state acid–base equilibria of **Ru(Hecip)** were studied by means of UV/Vis absorption spectrophotometric and spectrofluorimetric titrations, respectively, in a Britton–Robinson/DMF (40 mM H_3BO_3, 40 mM H_3PO_4, 40 mM CH_3COOH; v/v, 4:1) buffer solution containing NaCl (0.2 M). The UV/Vis and emission spectra were measured after each addition of the base (1 M NaOH). The emission spectra were collected without degassing the solutions at room temperature by excitation at the lowest-energy MLCT band at 530 nm.

TiO_2 Electrode Preparation: The mesoporous, nanocrystalline anatase TiO_2 particles were prepared by hydrolysis of titanium(IV) tetrabutoxide [$Ti(OC_4H_9)_4$] according to the general sol-gel method.[32] Nanoporous TiO_2 electrodes were prepared as follows. A colloidal suspension of TiO_2 particles was deposited on a transparent conductive FTO substrate pretreated according to the standard procedure.[37] The electrodes were dried at 100 °C for 30 min and then sintered in air for 30 min at 450 °C. The heated electrode was impregnated with 50 mM titanium tetrachloride aqueous solution at 70 °C for 30 min followed by heating at 450 °C once more for 30 min. The hot electrodes (ca. 80 °C) were immersed in a (2–3) × 10^{-4} M **Ru(Hecip)** solution in ethanol for 12–16 h. The **Ru(Hecip)**-coated electrodes were rinsed 5–6 times quickly with anhydrous ethanol and used as such for photovoltaic measurements. The amount of chemisorbed dye was determined by desorbing the complex from the TiO_2 film into a KOH (0.02 M) methanol solution, and measuring the absorption spectrum of the complex. The surface coverage (mol cm^{-2}) of the Ru^{II} sensitizers, Γ, was thus estimated.

Dye-Sensitized Solar Cell Fabrication: A **Ru(Hecip)**-coated TiO_2 film was used as a working electrode where the effective area for illumination was 0.14 cm^2, and these two electrodes were then clamped tightly using clips. One drop of the redox electrolyte (0.5 M LiI and 0.05 M I_2 in 50% acetonitrile and 50% PC) was then placed between the two electrodes and allowed to wet the surfaces of the electrodes by capillary action.

Photoelectrochemical Measurements: Photocurrent-voltage (*I-V*) curve measurements for the solar cells were performed by using a Keithley Model 2400 computer-controlled digital source meter under a 500 W xenon-light source that was focused to give 100 mW cm^{-2}, the equivalent of one sun unit at air mass 1.5. The photoelectrochemical data of the known reference dye **N3** were also measured under the same experimental conditions as those for **Ru(Hecip)** and were compared to each other. The plots of incident monochromatic photon-to-current conversion efficiencies (IPCEs) of the solar cells versus incident radiative wavelength were measured in a two-electrode system with a dye-coated TiO_2 film on FTO as a working electrode and a 200-nm-thick platinum film deposited on glass by sputtering as a counter electrode. The redox electrolyte consists of I_2 (0.05 M) and LiI (0.5 M) in 50% acetonitrile and 50% PC. A 500-W xenon lamp served as a light source in conjunction with a monochromator. The ultraviolet and infrared radiations were removed with a band pass filter (400–800 nm).

Light intensities were measured with a light gauge radiometer (FZ-A, Photoelectric Instrument Factory of Beijing Normal University). All the IPCEs were obtained with the same device and measurement procedure. The incident light intensities used for efficiency determination were uncorrected for the light reflection, scattering, and absorption by the glass sheet and the filtering effect by the electrolyte.

Supporting Information (see also the footnote on the first page of this article): Synthetic route to **Ru(Hecip)**, synthetic details of **Ru(Hecip)**, ^{1}H NMR spectrum of **Ru(Hecip)**, absorption spectra of **Ru(Hecip)** in ethanol and on the TiO_2 film, pH effects on the excitation spectra of **Ru(Hecip)** at λ_{em} = 780 nm and λ_{em} = 660 nm, and pH effects on the emission spectra at λ_{ex} = 470 nm.

Acknowledgments

The authors would like to thank the National Natural Science Foundation (20771016 and 90401007), Beijing Natural Science Foundation (2072011), Research Fund for the Doctoral Program of Higher Education (20060027002), and Analytical and Measurements Fund of Beijing Normal University for financial support.

[1] a) B. O'Regan, M. Grätzel, *Nature* **1991**, *353*, 737–740; b) C. A. Bignozzi, R. Argazzi, C. J. Kleverlaan, *Chem. Soc. Rev.* **2000**, *29*, 87–96; c) N. Robertson, *Angew. Chem. Int. Ed.* **2006**, *45*, 2338–2345; d) S. Hattori, Y. Wada, S. Yanagida, S. Fukuzumi, *J. Am. Chem. Soc.* **2005**, *127*, 9648–9654; e) N. Robertson, *Angew. Chem. Int. Ed.* **2008**, *47*, 1012–1014; f) M. Grätzel, *Inorg. Chem.* **2005**, *44*, 6841–6851; g) A. Reynal, A. Forneli, E. Martinez-Ferrero, A. Sanchez-Diaz, A. Vidal-Ferran, E. Palomares, *Eur. J. Inorg. Chem.* **2008**, 1955–1958.

[2] a) M. K. Nazeeruddin, P. Péchy, T. Renouard, S. M. Zakeeruddin, R. Humphry-Baker, P. Comte, P. Liska, L. Cevey, E. Costa, V. Shklover, L. Spiccia, G. B. Deacon, C. A. Bignozzi, M. Grätzel, *J. Am. Chem. Soc.* **2001**, *123*, 1613–1624; b) S. R. Jang, C. C. Lee, H. B. Choi, J. J. Ko, J. Lee, R. Vittal, K. J. Kim, *Chem. Mater.* **2006**, *18*, 5604–5608; c) I. Jung, H. Choi, J. K. Lee, K. H. Song, S. O. Kang, J. Ko, *Inorg. Chim. Acta* **2007**, *360*, 3518–3524; d) B. Liu, W. Zhu, W. Wu, K. M. Ri, H. Tian, *J. Photochem. Photobio. A: Chem.* **2008**, *194*, 268–274; e) S. A. Haque, S. Handa, K. Peter, E. Palomares, M. Thelakkat, J. R. Durrant, *Angew. Chem. Int. Ed.* **2005**, *44*, 5740–5744.

[3] a) M. J. Scott, J. J. Nelson, S. Caramori, C. A. Bignozzi, C. M. Elliott, *Inorg. Chem.* **2007**, *46*, 10071–10078; b) D. Kuciauskas, M. S. Freund, H. B. Gray, J. R. Winkler, N. S. Lewis, *J. Phys. Chem. B* **2001**, *105*, 392–403; c) R. Argazzi, G. Larramona, C. Contado, C. A. Bignozz, *J. Photochem. Photobio. A: Chem.* **2004**, *164*, 15–21.

[4] a) S. Ferrere, B. A. Gregg, *J. Am. Chem. Soc.* **1998**, *120*, 843–844; b) J. E. Monat, J. K. McCusker, *J. Am. Chem. Soc.* **2000**, *122*, 4092–4097.

[5] a) L. Schmidt-Mende, U. Bach, R. Humphry-Baker, T. Horiuchi, H. Miura, S. Ito, S. Uchida, M. Grätzel, *Adv. Mater.* **2005**, *17*, 813–815; b) R. K. Chen, X. C. Yang, H. N. Tian, L. C. Sun, *J. Photochem. Photobio. A: Chem.* **2007**, *189*, 295–300; c) W. H. Howie, F. Claeyssens, H. Miura, L. M. Peter, *J. Am. Chem. Soc.* **2008**, *130*, 1367–1375.

[6] a) F. Odobel, E. Blart, M. Lagree, M. Villieras, H. Boujtita, N. El Murr, S. Caramori, C. A. Bignozzi, *J. Mater. Chem.* **2003**, *13*, 502–510; b) W. M. Campbell, K. W. Jolley, P. Wagner, K. Wagner, P. J. Walsh, K. C. Gordon, L. Schmidt-Mende, M. K. Nazeeruddin, Q. Wang, M. Grätzel, D. L. Officer, *J. Phys. Chem. C* **2007**, *111*, 11760–11762.

[7] M. K. Nazeeruddin, R. Humphry-Baker, P. Liska, M. Grätzel, *J. Phys. Chem. B* **2003**, *107*, 8981–8987.

[8] Y. J. Hou, P. H. Xie, Z. Jing, B. W. Zhang, Y. Cao, X. R. Xiao, W. B. Wang, *Inorg. Chem.* **1999**, *38*, 6320–6322.

[9] a) N. Hirata, J. J. Lagref, E. J. Palomares, J. R. Durrant, M. K. Nazeeruddin, M. Grätzel, D. Di Censo, *Chem. Eur. J.* **2004**, *10*, 595–602; b) K. Hara, H. Horiuchi, R. Katoh, L. P. Singh, H. Sugihara, K. Sayama, S. Murata, M. Tachiya, H. Arakawa, *J. Phys. Chem. B* **2002**, *106*, 374–379; c) Y. C. Hsu, H. G. Zheng, J. T. Lin, K. C. Ho, *Sol Energy Mater. Sol Cells* **2005**, *87*, 357–367; d) M. K. Nazeeruddin, C. Klein, P. Liska, M. Grätzel, *Coord. Chem. Rev.* **2005**, *249*, 1460–1467.

[10] a) A. Higuchi, H. Inada, Y. Shirota, *Adv. Mater.* **1991**, *3*, 549–550; b) K. K. Tamura, N. Peyghambrian, A. B. Padias, H. K. Hall, *Phys. Rev. B* **1993**, *48*, 10710–10714; c) Z. Peng, Z. Bao, L. Yu, *J. Am. Chem. Soc.* **1994**, *116*, 6003–6004; d) A. van Dijken, J. J. A. M. Bastiaansen, N. M. M. Kiggen, B. M. W. Langeveld, C. Rothe, A. Monkman, I. Bach, P. Stossel, K. Brunner, *J. Am. Chem. Soc.* **2004**, *126*, 7718–7727; e) J. Y. Li, D. Liu, Y. Q. Li, C. S. Lee, H. L. Kwong, S. Lee, *Chem. Mater.* **2005**, *17*, 1208–1212.

[11] a) H. Hoegl, *J. Phys. Chem.* **1965**, *69*, 755–766; b) G. E. Johnston, *J. Phys. Chem.* **1974**, *78*, 1512–1521; c) L. E. Nitzche, C. Chabalowski, R. E. Christofferson, *J. Am. Chem. Soc.* **1978**, *100*, 1371–1378; d) S. Grigalevicius, J. V. Grazulevicius, V. Gaidelis, V. Jankauskas, *Polymer* **2002**, *43*, 2603–2608; e) M. Schaerlaekens, E. Hendrickx, A. Hameurlaine, W. Dehaen, A. Persoons, *Chem. Phys.* **2002**, *277*, 43–52; f) S. I. van Dijk, C. P. Groen, F. Hartl, A. M. Brouwer, J. W. Verhoeven, *J. Am. Chem. Soc.* **1996**, *118*, 8425–8432; g) Z. R. Grabowski, K. Rotkiewicz, *Chem. Rev.* **2003**, *103*, 3899–4032.

[12] a) Y. Zhang, L. Wang, T. Wada, H. Sasabe, *Macromol. Chem. Phys.* **1996**, *197*, 1877–1888; b) J. Wagner, J. Pielichowski, A. Hinsch, K. Pielichowski, D. Bogdał, M. Pajda, S. S. Kurek, A. Burczyk, *Synth. Met.* **2004**, *146*, 159–165; c) M. Guan, Z. Q. Bian, H. Xin, C. H. Huang, *New J. Chem.* **2003**, *27*, 1731–1734; d) M. Guan, Z. Q. Bian, Y. F. Zhou, F. Y. Li, Z. J. Li, C. H. Huang, *Chem. Commun.* **2003**, 2708–2709.

[13] a) H. Xin, M. Sun, K. Z. Wang, Y. A. Zhang, L. P. Jin, C. H. Huang, *Chem. Phys. Lett.* **2004**, *388*, 55–57; b) H. Xin, F. Y. Li, M. Guan, C. H. Huang, M. Sun, K. Z. Wang, Y. A. Zhang, L. P. Jin, *J. Appl. Phys.* **2003**, *94*, 4729–4731; c) F. R. Liu, K. Z. Wang, G. Y. Bai, Y. A. Zhang, L. H. Gao, *Inorg. Chem.* **2004**, *43*, 1799–1806; d) Y. Y. Lü, L. H. Gao, M. J. Han, K. Z. Wang, *Eur. J. Inorg. Chem.* **2006**, *430*, 430–436; e) M. Sun, H. Xin, Y. A. Zhang, K. Z. Wang, L. P. Jin, C. H. Huang, *Huaxue Xuebao (in Chinese)* **2003**, *61*, 1323–1325.

[14] a) A. C. Ribou, T. Wada, H. Sasabe, *Inorg. Chim. Acta* **1999**, *288*, 134–141; b) N. D. McClenaghan, R. Passalacqua, F. Loiseau, S. Campagna, B. Verheyde, A. Hameurlaine, W. Dehaen, *J. Am. Chem. Soc.* **2003**, *125*, 5356–5365; c) S. H. Hwang, P. Wang, C. N. Moorefield, L. A. Godinez, J. Manriquez, E. Bustos, G. R. Newkome, *Chem. Commun.* **2005**, 4672–4674; d) K. Peter, M. Thelakkat, *Macromolecules* **2003**, *36*, 1779–1785; e) K. Peter, H. Wietasch, B. Peng, M. Thelakkat, *Appl. Phys. A* **2004**, *79*, 65–71; f) C. Pérez León, L. Kador, B. Peng, M. Thelakkat, *J. Phys. Chem. B* **2005**, *109*, 5783–5789.

[15] a) R. Argazzi, C. A. Bignozzi, T. A. Heimer, F. N. Castellano, G. J. Meyer, *J. Am. Chem. Soc.* **1995**, *117*, 11815–11816; b) C. S. Karthikeyan, H. Wietasch, M. Thelakkat, *Adv. Mater.* **2007**, *19*, 1091–1095; c) S. H. Fan, W. C. Yang, K. Z. Wang, *Huaxue Xuebao (in Chinese)* **2008**, *66*, 690–696; d) When we were preparing this revised manuscript two carbazole-containing Ru^{II} complexes were reported: X. H. Li, J. Gui, H. Yang, W. J. Wu, F. Y. Li, *Inorg. Chim. Acta* **2008**, *361*, 2835; C. Y. Chen, J. G. Chen, S. J. Wu, J. Y. Li, C. G. Wu, K. C. Ho, *Angew. Chem. Int. Ed.* **2008**, *47*, 7342–7345.

[16] a) M. A. Haga, *Inorg. Chim. Acta* **1983**, *75*, 29–35; b) T. Ohno, K. Nozaki, M. Haga, *Inorg. Chem.* **1992**, *31*, 548–555; c) M. Haga, M. M. Ali, S. Koseki, K. Fujimoto, A. Yoshimura, K. Nozaki, T. Ohno, K. Nakajima, D. J. Stufkens, *Inorg. Chem.* **1996**, *35*, 3335–3347; d) M. J. Han, Z. M. Duan, Q. Hao, K. Z. Wang, *J. Phys. Chem. C* **2007**, *111*, 16577–16585; e) M. J. Han, L. H. Gao, Y. Y. Lü, K. Z. Wang, *J. Phys. Chem. B* **2006**, *110*,

2364–2371; f) M. J. Han, L. H. Gao, K. Z. Wang, *New J. Chem.* **2006**, *30*, 208–214; g) G. Y. Bai, B. Dong, K. Z. Wang, L. P. Jin, L. H. Gao, *J. Inorg. Biochem.* **2004**, *98*, 2011–2015; h) G. Y. Bai, K. Z. Wang, Z. M. Duan, L. H. Gao, *J. Inorg. Biochem.* **2004**, *98*, 1017–1022; i) K. Z. Wang, L. H. Gao, G. Y. Bai, L. P. Jin, *Inorg. Chem. Commun.* **2002**, *5*, 841–843; j) H. Cao, B. H. Ye, H. Li, R. H. Li, J. Y. Zhou, L. N. Ji, *Polyhedron* **2000**, *19*, 1975–1983; k) H. Cao, B. H. Ye, Q. L. Zhang, L. N. Ji, *Inorg. Chem. Commun.* **1999**, *2*, 338–340.

[17] S. M. Zakeeruddin, M. K. Nazeeruddin, R. Humphry-Baker, M. Grätzel, *Inorg. Chem.* **1998**, *37*, 5251–5259.

[18] A. Juris, V. Balzani, F. Barigelletti, S. Campagna, P. Belser, A. von Zelewsky, *Coord. Chem. Rev.* **1988**, *84*, 85–277.

[19] A. Islam, H. Sugihara, H. Arakawa, *J. Photochem. Photobio. A: Chem.* **2003**, *158*, 131–138.

[20] a) M. K. Nazeeruddin, S. M. Zakeeruddin, J. J. Lagref, P. Liska, P. Comte, C. Barolo, G. Viscardi, K. Schenk, M. Grätzel, *Coord. Chem. Rev.* **2004**, *248*, 1317–1328; b) L. C. T. Shoute, G. R. Loppnow, *J. Am. Chem. Soc.* **2003**, *125*, 15636–15646; c) D. Martineau, M. Beley, P. C. Gros, S. Cazzanti, S. Caramori, C. A. Bignozzi, *Inorg. Chem.* **2007**, *46*, 2272–2277.

[21] T. Shimidzu, T. Iyoda, K. Izaki, *J. Phys. Chem.* **1985**, *89*, 642–645.

[22] M. K. Nazeeruddin, K. Kalyanasundaram, *Inorg. Chem.* **1989**, *28*, 4251–4259.

[23] M. K. Nazeeruddin, E. Müller, R. Humphry-Baker, N. Vlachopoulos, M. Grätzel, *J. Chem. Soc., Dalton Trans.* **1997**, 4571–4578.

[24] J. V. Houten, R. J. Watts, *J. Am. Chem. Soc.* **1976**, *98*, 4853–4858.

[25] a) T. Gunnlaugsson, J. P. Leonard, K. Snchal, A. J. Harte, *J. Am. Chem. Soc.* **2003**, *125*, 12062–12063; b) L. Stryer, *Biochemistry*, 3rd ed.; Freeman: New York, **1988**; c) L. Fabbrizzi, F. Gatti, P. Pallavicini, L. Parodi, *New J. Chem.* **1998**, *22*, 1403–1407; d) P. Pallavicini, V. Amendola, C. Massera, E. Mundum, A. Taglietti, *Chem. Commun.* **2002**, 2452–2453; e) E. C. Glazer, D. Magde, Y. Tor, *J. Am. Chem. Soc.* **2007**, *129*, 8544–8551; f) E. C. Glazer, D. Magde, Y. Tor, *J. Am. Chem. Soc.* **2005**, *127*, 4190–4192; g) T. E. Keyes, C. O'Connor, J. G. Vos, *Chem. Commun.* **1998**, 889–890; h) T. E. Keyes, C. O'Connor, U. O'Dwyer, C. G. Coates, P. Callaghan, J. J. McGarvey, J. G. Vos, *J. Phys. Chem. A* **1999**, *103*, 8915–8920; i) L. Song, J. Feng, X. Wang, J. Yu, Y. Hou, P. Xie, B. Zhang, J. Xiang, X. Ai, J. Zhang, *Inorg. Chem.* **2003**, *42*, 3393–3395; j) R. L. Blakley, M. L. Myrick, M. K. DeArmond, *J. Am. Chem. Soc.* **1986**, *108*, 7843–7844; k) R. L. Blakley, M. K. DeArmond, *J. Am. Chem. Soc.* **1987**, *109*, 4895–4901; l) The solvent contribution to the dual emission has been excluded by using freshly distilled solvent and by checking the pH-dependent emission spectra of the blank solution.

[26] a) E. V. Donckt, *Progress in Reaction Kinetics*, 5th ed., (Ed.: G. Poter), Pergamon Press: Oxford, England, **1970**; b) G. Y. Zheng, Y. Wang, D. P. Rillema, *Inorg. Chem.* **1996**, *35*, 7118–7123.

[27] a) A. Fillinger, B. A. Parkinson, *J. Electrochem. Soc.* **1999**, *146*, 4559–4564; b) C. P. León, L. Kador, B. Peng, M. Thelakka, *J. Phys. Chem. B* **2006**, *110*, 8723–8730; c) H. Yi, J. A. Crayston, J. T. Irvine, *Dalton Trans.* **2003**, 685–691; d) K. Murakoshi, G. Kano, Y. Wada, S. Yanagida, H. Miyazaki, M. Matsumoto, S. Murasawa, *J. Electroanal. Chem.* **1995**, *396*, 27–34; e) M. Nara, H. Torii, M. Tasumi, *J. Phys. Chem.* **1996**, *100*, 19812–19817; f) N. W. Duffy, K. D. Dobson, K. C. Gordon, B. H. Robinson, A. J. NcQuillan, *Chem. Phys. Lett.* **1997**, *266*, 451–455; g) K. S. Finnie, J. R. Bartlett, J. L. Woolfrey, *Langmuir* **1998**, *14*, 2744–2749.

[28] G. J. Samuels, T. J. Meyer, *J. Am. Chem. Soc.* **1981**, *103*, 307–312.

[29] G. Wolfbauer, A. M. Bond, G. B. Deacon, D. R. MacFarlane, L. Spiccia, *J. Am. Chem. Soc.* **2000**, *122*, 130–142.

[30] F. T. Kong, S. Y. Dai, K. J. Wang, *Chin. J. Chem.* **2007**, *25*, 168–171.

[31] J. Bisquert, D. Cahen, G. Hodes, S. Rühle, A. Zaban, *J. Phys. Chem. B* **2004**, *108*, 8106–8118.

[32] M. K. Nazeeruddin, A. Kay, I. Rodicio, R. Humphry-Baker, E. Müller, P. Liska, N. Vlachopoulos, M. Grätzel, *J. Am. Chem. Soc.* **1993**, *115*, 6382–6390.

[33] N. Garelli, P. Vierling, *J. Org. Chem.* **1992**, *57*, 3046–3051.

[34] I. P. Evans, A. Spencer, G. Wilkinson, *J. Chem. Soc., Dalton Trans.* **1973**, *2*, 204–209.

[35] M. K. Nazeeruddin, S. M. Zakeeruddin, R. Humphry-Baker, M. Jirousek, P. Liska, N. Vlachopoulos, V. Shklover, C. H. Fischer, M. Grätzel, *Inorg. Chem.* **1999**, *38*, 6298–6305.

[36] a) T. Gennett, D. F. Milner, M. J. Weaver, *J. Phys. Chem.* **1985**, *89*, 2787–2794; b) C. J. Cunha, E. S. Dodsworth, M. A. Monteiro, A. B. P. Lever, *Inorg. Chem.* **1999**, *38*, 5399–5409.

[37] Z. S. Wang, K. Hara, Y. Danoh, C. Kasada, A. Shinpo, S. Suga, H. Arakawa, H. Sugihara, *J. Phys. Chem. B* **2005**, *109*, 3907–3914.

Received: June 14, 2008
Published Online: December 19, 2008

